molecular pharmaceutics

ARTICLE

pubs.acs.org/molecularpharmaceutics

# Differences in DNA Condensation and Release by Lysine and Arginine Homopeptides Govern Their DNA Delivery Efficiencies

Anita Mann,[†] Garima Thakur,[†] Vasundhara Shukla,[†] Anand Kamal Singh,[†] Richa Khanduri,[†] Rangeetha Naik,[†] Yang Jiang,[‡] Namita Kalra,[§] B. S. Dwarakanath,[§] Ulo Langel,[‡] and Munia Ganguli*[,†]

[†]Institute of Genomics and Integrative Biology (CSIR), Mall Road, Delhi 110007, India

[§]Institute of Nuclear Medicine and Allied Sciences (DRDO), Ministry of Defence, Government of India, Timarpur, Lucknow Road, Delhi 110007, India

[‡]Department of Neurochemistry, University of Stockholm, S-10691, Stockholm, Sweden

Supporting Information

**ABSTRACT:** Designing of nanocarriers that can efficiently deliver therapeutic DNA payload and allow its smooth intracellular release for transgene expression is still a major constraint. The optimization of DNA nanocarriers requires thorough understanding of the chemical and structural characteristics of the vector−nucleic acid complexes and its correlation with the cellular entry, intracellular state and transfection efficiency. L-Lysine and L-arginine based cationic peptides alone or in conjugation with other vectors are known to be putative DNA delivery agents. Here we have used L-lysine and L-arginine homopeptides of three different lengths and probed their DNA condensation and release properties by using a multitude of biophysical techniques including fluorescence spectroscopy, gel electrophoresis and atomic force microscopy. Our results clearly showed that although both lysine and arginine based homopeptides condense DNA via electrostatic interactions, they follow different pattern of DNA condensation and release *in vitro*. While lysine homopeptides condense DNA to form both monomolecular and multimolecular complexes and show differential release of DNA *in vitro* depending on the peptide length, arginine homopeptides predominantly form multimolecular complexes and show complete DNA release for all peptide lengths. The cellular uptake of the complexes and their intracellular state (as observed through flow cytometry and fluorescence microscopy) seem to be controlled by the peptide chemistry. The difference in the transfection efficiency of lysine and arginine homopeptides has been rationalized in light of these observations.

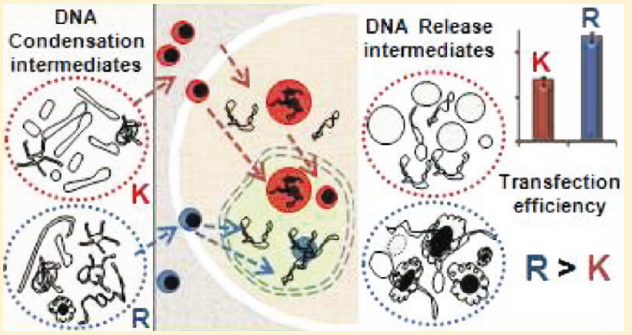


**KEYWORDS:** nonviral gene delivery, cationic peptides, DNA condensation, atomic force microscopy, condensation−release balance, structure−activity correlation

## INTRODUCTION

Nanocarriers for delivery of therapeutic DNA into cells have been pivotal in developing new paradigms in gene therapy for treating and controlling diseases ranging from simple monogenic disorders to complex diseases like cancer.[1] Viruses have been extensively used for this purpose since, as obligate intracellular parasites, they are naturally evolved to evade biological barriers during cellular delivery. However, they suffer from nondesirable side effects like gene conversion and fatal immune responses as well as limited DNA carrying capacity. Nonviral chemical vectors present a more viable alternative as they are less toxic, easy to synthesize and functionalize and do not induce specific immune responses. A chemical DNA delivery vector should have DNA efficiently packaged by a cationic molecule, remain stable and inert during circulation in the body, reach the target cell through the extracellular matrix and be able to overcome the intracellular barriers like internalization and intracellular trafficking, escape from the endosomes, entry to nucleus and efficient gene transcription/expression.[2] The development of such vectors based on rational design requires integration of multiple features to address each of these barriers. Although a plethora of vectors based on liposomes and cationic polymers have been developed, their inability to efficiently overcome many of these biological barriers results in poor efficacy.[3] Peptides provide a lucrative alternative as different classes of peptides can overcome both extracellular and intracellular barriers such as cell targeting, DNA condensation, membrane translocation, endosomal escape and nuclear delivery.[4−6] Additionally, they are easy to synthesize and provide flexibility in design by conjugation with functional moieties as well as other nonviral systems like lipids and polymers to create modular systems.

**Received:** February 21, 2011
**Accepted:** July 24, 2011
**Revised:** May 13, 2011
**Published:** July 25, 2011





dx.doi.org/10.1021/mp2000814 | *Mol. Pharmaceutics* 2011, 8, 1729–1741

Both lysine and arginine based peptides have been used for efficient packaging of DNA into nanoparticles to prevent cellular degradation and improve DNA availability. Short DNA condensing lysine peptides like YKAKnWK, $CWK_{18}$ and AlkCWKn ($n$ = 3−36), $K_8$ and $K_{16}$ have been studied where the role of size and stability of their condensates on transfection efficiency has been demonstrated.[7−10] Cell penetrating ability of arginine rich peptides has also fetched attention where oligoarginines, HIV-1 TAT and its derivatives, antennapedia etc. have demonstrated their potential in gene delivery.[11−13] Moreover in conjugation with other agents, e.g. grafting of arginine residues to PAMAM dendrimers, stearylation of oligoarginine and incorporation of $R_8$ into multifunctional envelope-type nanodevice-like system, presence of arginines has improved DNA delivery efficiency to levels comparable to that of commercially available transfection reagents and adenoviruses *in vitro*.[14−16]

Although the efficient condensation of DNA by such cationic moieties is indispensable, emerging evidence also indicates that very strong packaging of DNA leads to inefficient intracellular release and reduced efficacy.[17] For example a quantitative comparison of the intracellular trafficking and postnuclear events between adenoviral and lipoplex systems has demonstrated that although lipofectamine can deliver DNA to the nucleus with a speed comparable to that of adenovirus, it requires 3-fold higher dose of DNA to exhibit a similar level of transfection as the adenovirus because of poor accessibility of DNA from the lipofectamine−DNA complex to the transcription machinery.[18] Similarly, in the case of poly-L-lysine containing 19−180 amino acids, plasmid unpackaging has been found to be a barrier for the longer polymers and short-term gene expression is significantly enhanced by using the shorter polycations.[19] Short oligomeric chitosans and low molecular weight poly(ethyleneimine) have been shown to be effective carriers as compared to their high molecular weight counterparts since their condensates can easily disassemble at appropriate compartments inside the cells allowing higher DNA accessibility.[20,21] Thus a DNA delivery carrier should possess the right balance between effective DNA packaging and efficient intracellular disassembly when required for gene expression. The condensation and release balance is likely to be dictated by the chemical and structural characteristics of DNA delivery agent as well as its nature of interaction with DNA i.e. mechanism and efficiency of DNA assembly.

Although lysine and arginine based peptides alone or in conjugation with other functional moieties have been used for DNA delivery, an extensive comparison of their DNA condensation and release characteristics and its effect on cellular delivery efficiency is not well-established. Such information is critical for further development of cationic peptide based DNA delivery agents. In this work we have taken lysine and arginine homopeptides and studied the effect of peptide length (containing 9, 12, and 16 amino acids) and peptide chemistry on DNA condensation *in vitro* and observed its effect on transfection efficiency. Our results indicate that DNA delivery efficiency of both classes of peptides increases with increase in peptide length and the efficacy of arginine peptides is higher than that of lysine peptides at any length. We observed that there are significant differences in DNA condensation and *in vitro* and intracellular release mechanisms between the lysine and arginine peptide−DNA complexes which can account for the difference in transfection efficiency. These observations indicate toward the obvious advantage of using arginine over lysine in a DNA condensation moiety of nonviral gene delivery systems.

## METHODS

**Chemicals Used.** All the chemicals used were purchased from Sigma-Aldrich unless stated otherwise.

**Plasmid DNA (pDNA) Isolation.** The plasmids pEGFP-C1, 4.7 Kb (Clonetech) encoding green fluorescent protein (GFP) and pMIR-REPORT Luciferase, 6.47 Kb (Ambion) encoding firefly luciferase were employed in the current study. Both expression vectors have the human cytomegalovirus immediate early promoter and were amplified in the DH5-α strain of *Escherichia coli*. The pDNA was purified using EndoFree Plasmid Maxi Kit (Qiagen; 12362). The purity and concentration of pDNA were determined by the 260/280 UV absorbance ratio, and plasmid integrity was determined by agarose gel electrophoresis and restriction enzyme digestion.

**Peptide Synthesis.** The peptides, either unlabeled or labeled with fluorescein isothiocyanate (FITC), were custom synthesized (>95% purity) by G L Biochem (Shanghai) Ltd. The peptide sequences include the following: $K_9$, 9-mer L-lysine; $K_{12}$, 12-mer L-lysine; $K_{16}$,16-mer L-lysine; $R_9$, 9-mer L-arginine; $R_{12}$, 12-mer L-arginine; $R_{16}$, 16-mer L-arginine. The arginine peptides were also synthesized in the laboratory using Fmoc chemistry. The peptides were dissolved in deionized water at a concentration of 5 mg/mL and stored in small aliquots at −80 °C. Repeated freez−thaw of the peptides was strictly avoided.

**Preparation of the Peptide−pDNA Complex (Polyplex).** Peptide−pDNA complexes (referred to as polyplexes in the text) were prepared at different charge ratios expressed as peptide nitrogen per nucleic acid phosphate (N/P) or as $Z$ (±). The pDNA stock was diluted to a concentration of (20−40) ng/μL and added dropwise to an equal volume of the appropriate peptide dilutions while vortexing, as already reported.[22,23]

**Cell Culture and Transfection.** Chinese hamster ovary cells (CHO-K1) and all GAG deficient CHO mutant cells (pgsA-745) were maintained in Ham's F-12K media whereas adenocarcinomic human alveolar basal epithelial cells (A-549) and breast cancer cells, Michigan Cancer Foundation-7 (MCF-7), were cultured in Dulbecco's modified Eagle medium (DMEM), both supplemented with 10% (v/v) fetal bovine serum (Life Technologies, USA), at 37 °C and 5% $CO_2$ in humidified incubator.

Cells were seeded in a 24-well plate format, and the experiment was done at 70% confluency after 24 h. Polyplexes were prepared at different charge ratios $Z$ (±) with final pDNA concentration of 20 ng/μL (pMIR-Report luciferase) and incubated for one hour. 100 μL of polyplex (2 μg of pDNA/well) was added to cells with and without chloroquine (100 μM final) in serum free media (OptiMEM). After 5 h of incubation, the media containing polyplexes was aspirated and cells were rinsed with 1× PBS (pH 7.4) and finally supplemented with complete growth medium. After 24 h of transfection, cells were lysed with 100 μL of cell culture lysis buffer (1× CCLR, Promega) and luciferase activity was measured by mixing luciferase assay substrate (Promega) and cell lysate in 1:1 ratio using a luminometer (Berthold Detection System, Germany). Transfection efficiency was normalized with total protein content of the cells, estimated using bicinchoninic acid assay (BCA). Transfection efficiency is presented as mean value ± standard deviation (SD) of three independent experiments, each performed in duplicate.

**Agarose Gel Assays.** The electrophoretic mobility of the polyplexes prepared at different charge ratios $Z$ (±) ranging from 0 to 5 was studied using agarose gel electrophoresis. 20 μL of the polyplex having 200 ng of total pDNA was loaded in each case

onto 1% agarose gel containing ethidium bromide. Electrophoresis was carried out at 100 V in 1× TAE buffer (pH 7.4) for 30 min.

For DNA release assay the polyplexes formed at charge ratio $Z$ (±) of 10 were treated for 30 min with increasing amount of anionic agents, dextran sulfate (D6924, MW ∼ 10,000 Da) and heparin (H3149-100KU) in wt/wt (anionic agent/peptide) ratios ranging from 0.25:1 to 2:1 and analyzed on 1% agarose gel. The amount of the pDNA released from the polyplexes was compared with that of the native uncomplexed pDNA.

**Fluorimetry Experiments.** DNA condensation was measured from the inhibition of DNA-intercalated EtBr fluorescence signal in the presence of peptides. The assay was carried out in black 96-well format plates (nunc) where 10 μL of EtBr (4.22 ng/μL) and 20 μL of pDNA (20 ng/μL) i.e., one EtBr molecule per 6 base pairs of pDNA, was dispensed in each well and incubated in the dark for 5 min at room temperature. 20 μL of peptide solution corresponding to different charge ratios was subsequently added. Two controls were also prepared where pDNA with EtBr and only EtBr were used. Further the plate was incubated for 15 min in the dark and fluorescence was recorded using 535 SL EXP 1 excitation and 595 SL EMP 1 emission filters (Beckman Coulter plate reader, DTX 880, USA). The fluorescence values of pDNA with EtBr were taken as maximum, i.e. 100%, and the relative percentage inhibition in fluorescence signal was calculated at increasing charge ratios and plotted as percentage of maximum (% of Max).

For DNA release assay the polyplexes (in each case) were prepared at charge ratio 10 and incubated for 30 min at room temperature. Meanwhile glycosaminoglycans (GAGs, heparin or dextran sulfate) were added to the different wells of the black 96-well plate at increasing amounts, followed by addition of 20 μL of incubated polyplex and EtBr (at the same concentration as for the condensation assay) and volume was made up to 60 μL with MQ water. Three controls, namely, pDNA with EtBr, EtBr alone and GAGs with EtBr, were also prepared. The fluorescence was recorded as described in the earlier section. The fluorescence value of pDNA control was taken as 100%, and the relative percentage increase in fluorescence signal was calculated at increasing concentration of GAGs.

**Atomic Force Microscopy (AFM).** All AFM images were obtained using PicoSPM equipment (Molecular Imaging, AZ, USA). Imaging was performed in air using AAC mode to ensure minimum sample damage with scan speed of 1 line/s. Cantilevers (Molecular Imaging), TypeII, Si, 225 μm long, resonance frequency of around 75 kHz and force constant of 2.8 N/m were used for imaging. Bare pDNA was imaged and dimensions of the individual molecules were measured as reported by us earlier.[22,23] The polyplexes were imaged by simply depositing 2 μL of the polyplex solution on freshly cleaved mica and drying it in air. For each sample 15 images (10 μm × 10 μm) were collected for analysis. The images were checked for nonuniformity due to loading and whenever there was an apparent variation among images of the same sample; experiments were repeated with fresh deposition on mica surface. Once image to image variation was ruled out, one representative image was chosen and image analysis (contour length and width measurements) was carried out using SPIP software. The proportion of complexes having different morphology were quantified by measuring the molecular dimensions of around 200−300 entities. Predominantly five different molecular morphologies were observed, and they were manually categorized based on their shape and dimensions as described in Results. For the DNA release experiment, 20 μL of polyplex at $Z$ (±) of 10 was prepared and incubated for 30 min. Dextran sulfate was then added to it in different wt/wt ratios and the mixture further incubated for 30 min before imaging. Control experiments were carried out by imaging peptide and dextran sulfate alone, pDNA with dextran sulfate and peptide with dextran sulfate at appropriate ratios.

**Measurement of Polyplex Size Using Dynamic Light Scattering (DLS).** The mean hydrodynamic diameter of selected lysine and arginine polyplexes prepared in deionized water was determined by dynamic light scattering (Zetasizer Nano ZS90, Malvern Instruments, U.K.) at a fixed angle of 90° at 25 °C. Size measurements were carried out for all the samples at charge ratio 10 (in automatic mode). At least 6 readings were recorded for each sample with replicates (each reading had 25 submeasurements).

**Plasmid Labeling.** Plasmid DNA (pEGFPC1) was labeled with tetramethyl Rhodamine (TM-Rh) using Label IT nucleic acid labeling kit (Cat No. MIR 7013, Mirus Bio, Madison, WI, USA) at 1:1 (v:w) ratio, i.e. 1 μL of labeling reagent for 1 μg of pDNA according to the manufacturer's protocol. The pDNA concentration was estimated using UV spectroscopy at 260 nm. The entire amount of pDNA used was labeled in one reaction to avoid the fluctuations in labeling densities among different labeling reactions.

**Flow Cytometry (FACS).** For measuring polyplex uptake, CHO-K1 cells were grown for 24 h in 24-well plate as mentioned above and fluorescently labeled polyplexes (having TM-Rh labeled pDNA) at $Z$ (±) of 10 were added to cells. After four hours of incubation, floating cells were collected and combined with the adherent cells. The adherent cells were washed twice with ice-cold 1× PBS (pH 7.4) having 1 mg/mL heparin to remove the extracellular bound polyplex, and with 0.4% trypan blue in 1× PBS to quench the extracellular fluorescence wherever required. Cells were collected by trypsinization (100 μL of 0.25% trypsin), pooled cells were washed with ice-cold 1× PBS supplemented with 1% BSA and resuspended in 500 μL of 1× PBS. Measurements were carried out on FACS-Calibur (Becton Dickinson, USA) using CellQuest Pro software. The TM-Rh labeled polyplexes were excited using 488 nm laser and detected with 585/42 nm (FL2) band-pass filter. A total of 10,000 events were acquired in each case, and the data shows the average of three independent experiments. Transfected cells with the unlabeled polyplexes were used to correct for the autofluorescence of cells.

For studying the intracellular state of the complex, dual labeled polyplexes (containing FITC labeled peptide and TM-Rh labeled pDNA) were used. The experimental and processing conditions were the same as above. Both FITC and TM-Rh labeled polyplex were excited using a 488 nm laser and detected with 530/30 nm (FL1) and 585/42 nm (FL2) band-pass filter respectively. Online compensation (FL2−87.1% FL1) was applied to remove the FITC emission from the TM-Rh channel (FL2) arising out of emission cross-talk of FITC. Negligible TM-Rh emission was observed in the FITC channel (FL1). The fluorescence resonance energy transfer (FRET) efficiency was calculated as $[(F_d - F_s)/F_d]$, where $F_d$ and $F_s$ are the mean fluorescence intensity of TM-Rh positive cells treated with the dual labeled and single labeled polyplexes respectively.[24]

**Fluorescence Microscopy.** CHO-K1 cells were seeded in ibidi 60 μ-Dish (Catalog No. 81156, Germany) at an initial

density of 120,000 cells. TM-Rh labeled polyplexes were prepared at $Z$ (±) of 10 and added to the cells (1 $\mu$g of pDNA per dish) in 400 $\mu$L of OptiMEM. After 4 h of incubation, the medium was removed and cells were washed at least 3 times with 1× PBS (+) containing 1 mg/mL heparin (to remove extracellular bound polyplexes from the cells). The imaging was done using a Nikon TiE motorized inverted fluorescence microscope equipped with a 63×, 1.4 NA plan apochromat oil immersion objective. The images were captured using monochrome camera (DS-Qi1MC), and false coloring was done using MetaMorph software (Molecular devices, USA). $Z$-Stack images of TM-Rh (excitation/emission 546/576 nm) were obtained along with differential interference contrast (DIC) images with a step size of 0.6 $\mu$m. The imaging parameters like lamp intensity, exposure time, LUT settings and contrast were kept constant for TM-Rh images for each sample. The $Z$ stack images were finally merged and processed for analysis. For analysis of microscopy images NIS viewer element (NIS-AR) software was used. 50−60 cells (each cell representing 1 ROI) showing red fluorescence were chosen randomly from DIC images, and ROI statistics were obtained. The sum intensity values of 50 ROIs (cells) were used for analysis and plotted in each case.

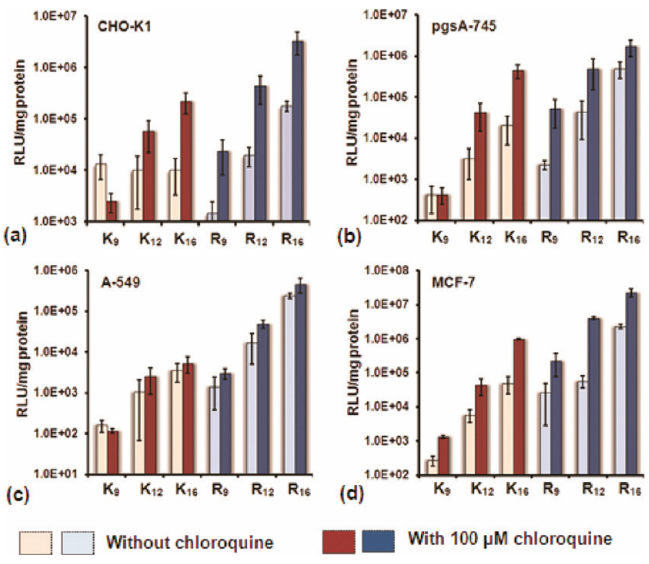


**Figure 1.** *In vitro* transfection of the luciferase gene into different cells: (a) CHO-K1, (b) pgsA-745, (c) A-549 and (d) MCF-7 by different polyplexes. Two $\mu$g of pDNA was used in each case. The average of three independent experiments is given where each experiment is performed in duplicate.

## RESULTS

**Transfection Efficiency of the Peptides in Different Cell Lines.** The transfection ability of all the six homopeptides was first tested as a function of charge ratio in CHO-K1 cells, and maximum efficiency was observed around charge ratio 10.0 (data not shown). The comparative transfection ability was examined at charge ratio 10.0 in CHO-K1, pgsA-745, A-549 and MCF-7 cell lines (Figure 1a−d). In all the cell lines, both lysine and arginine homopeptides show increase in transfection efficiency with increase in length. The transfection efficiency of the arginine peptides is better than that of the lysine peptides at any given length of the peptide in all the cell lines, clearly indicating that the two types of peptides behave differently. In all the cases, addition of endoosmotropic agent chloroquine substantially increases the transfection efficiency of all the polyplexes. This is because these polyplexes are likely to possess poor endosomal escape property and show significant DNA delivery efficiency only in the presence of an agent like chloroquine. However, the trend in transfection ability is the same in the presence and absence of chloroquine, which signifies that the inherent property of endosomal escape of both lysine and arginine homopeptides is similar. In order to rationalize the difference in transfection ability between lysine and arginine, we have studied their DNA condensation and release along with their cellular uptake and intracellular state.

**DNA Condensation Using Gel Retardation and Ethidium Bromide (EtBr) Exclusion Assay.** Gel retardation assay was carried out to determine the relative mobility of the polyplexes on condensation as a function of charge ratio (Figure 2a). All homopeptides efficiently retard the electrophoretic mobility of pDNA before or at a charge ratio 3.0. The shorter 9-mer peptides $K_9$ and $R_9$ show the strongest retardation which occurs at charge ratio of 1.75.

The condensation ability was also measured using EtBr assay (Figure 2b). Intercalation of EtBr into DNA increases the fluorescence quantum yield of the dye and thus gives 10-fold greater fluorescence emission. Presence of cationic moiety in the solution excludes EtBr from the DNA resulting in decrease in fluorescence intensity. All the peptides show maximum fluorescence drop at $Z$ (±) of 3.0. However, the overall drop in fluorescence intensity in the case of the arginine peptides is

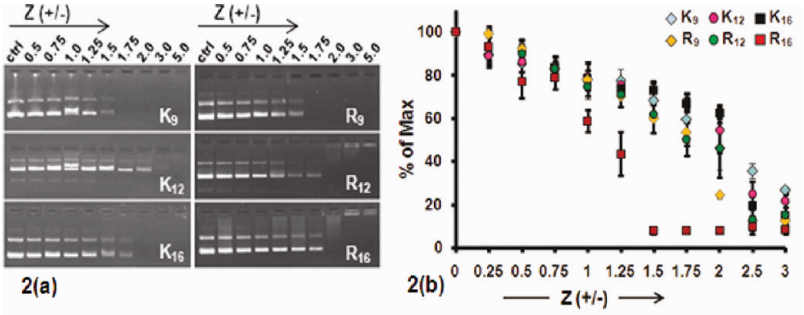


**Figure 2.** (a) Electrophoretic mobility shift assay of the lysine and arginine polyplexes. Lane 1: only plasmid DNA. Lanes 2−10 are the polyplexes formed at different charge ratios (0.5−5). (b) EtBr exclusion assay. The fluorescence of EtBr is inhibited with increasing amount of each peptide, i.e. with increase in charge ratio $Z$ (±). The fluorescence of uncomplexed DNA is set as 100%, and percent decrease in fluorescence at increasing charge ratio of different peptides is plotted.

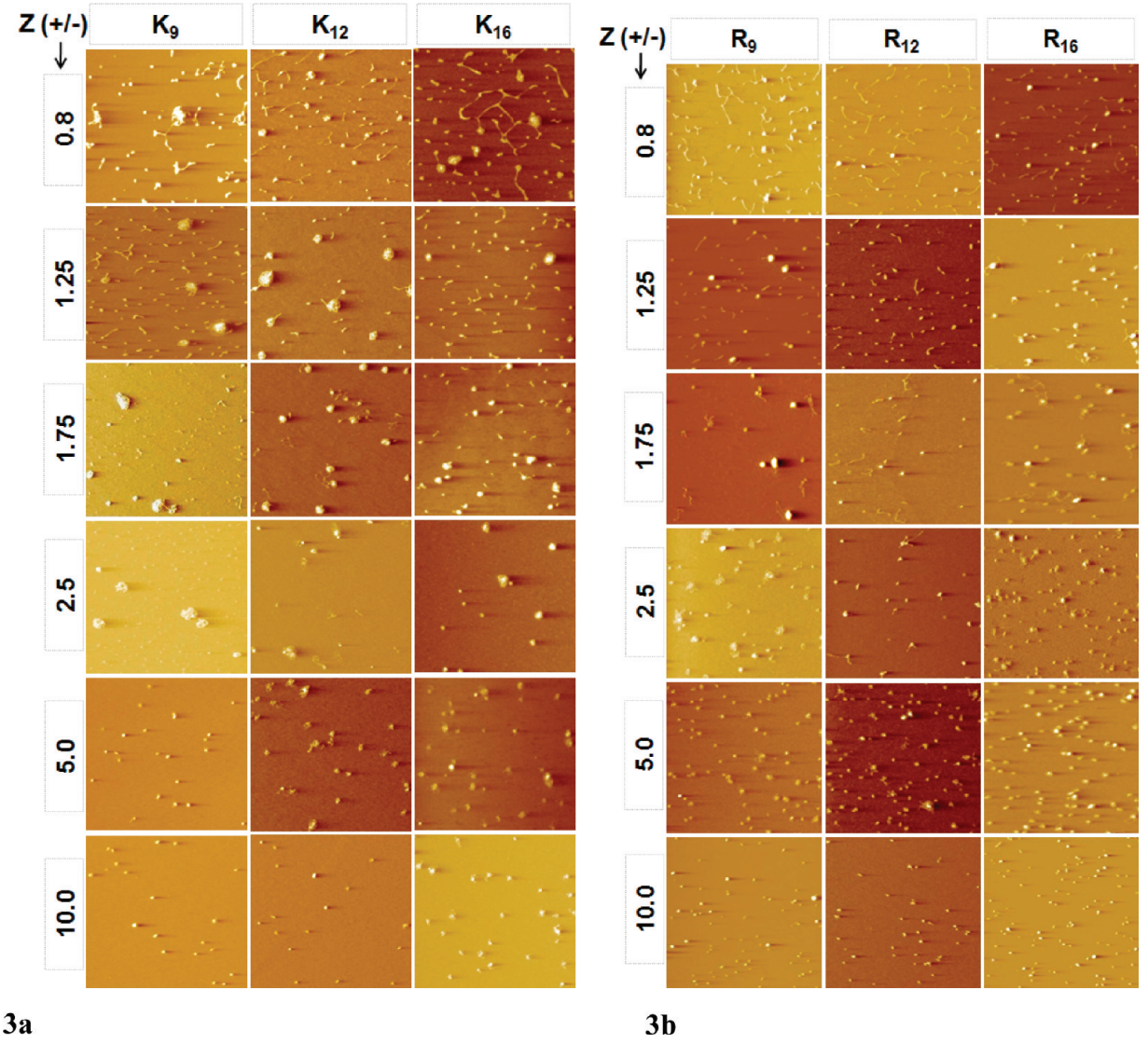


**Figure 3.** Representative AFM images (size 4 $\mu$m × 4 $\mu$m) of (a) lysine and (b) arginine polyplexes. Each column represents one peptide as mentioned in the figure, and each row designates the charge ratio at which the polyplex has been prepared.

more than that in the case of lysine peptides with $R_{16}$ showing the steepest drop in fluorescence. It may be noted that the partially complexed DNA molecules may not migrate in the gel since they are sufficiently packed to prevent migration but can be easily detected in a more sensitive assay like EtBr exclusion. Such variation between the two assays has also been observed by others.[25] These differences are more likely to happen when the packaging patterns vary and many different partially packed intermediates are formed at different charge ratios. Thus, although most of the peptides show complete retardation at charge ratio 2, the DNA-EtBr fluorescence is inhibited by only 50% except in the case of $R_{16}$. However, neither assay gives any direct insight into the morphology and sizes of the structures formed at different charge ratios. Atomic force microscopy was carried out for this purpose.

**Condensation Intermediates as Observed Using Atomic Force Microscopy (AFM).** AFM is an important tool to study the process of DNA condensation.[26,27] We have used AFM to gain mechanistic insight into the process of condensation of DNA using poly-L-ornithine and poly-L-lysine.[22,23] We have adopted the same methodology in this study. The representative AFM images of the polyplexes are shown in Figure 3a and 3b. From the

**Table 1. List of Different Categories of Molecules Seen in All the Polyplexes with Their Respective Representative AFM Image, Sketch and Symbol Used**

| Category | Representative AFM Images and their sketch |
|---|---|
| a; Linear rods : 70-100/40-60, {length/ width in nm} 100-200/30-60, 200-350/20-40 | |
| b; Interconnected linears, Flowers with long extensions | |
| c; Loose flowers ( > 200 nm ) | |
| d; Flowers, condensed particles (100-200 nm) | |
| e; Spheres (30-70 nm, 70-100 nm) | |
| f; Clumps | |

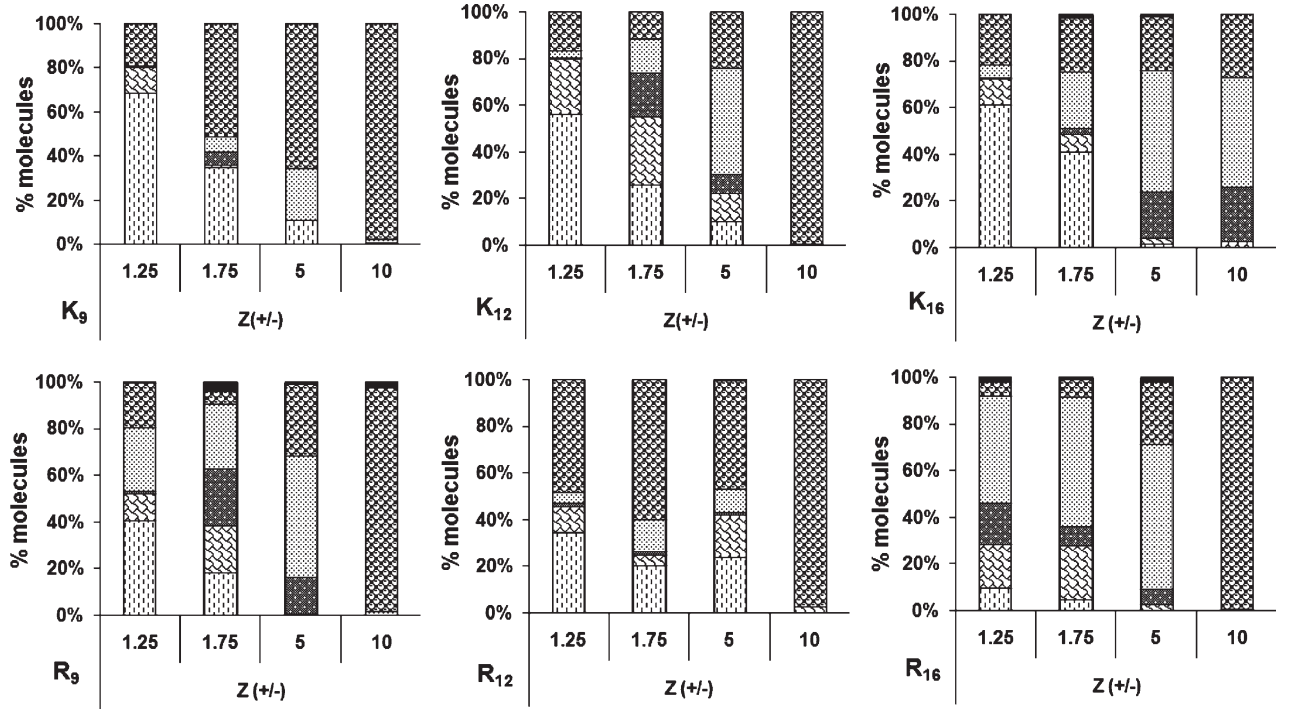


**Figure 4.** Population distribution of the different categories of molecules for the lysine (upper panel) and arginine polyplexes (lower panel) at different charge ratios. Different symbols in each bar represent one category of molecules. List of different categories of molecules seen in all the polyplexes with their respective representative AFM image, sketch and symbol used are described in Table 1.

AFM images, six types of structures were identified which are formed when DNA is condensed at each charge ratio. These are (a) linear, rodlike structures (of different lengths and widths, but shorter than the length of the pDNA); (b) interconnected linear structures where multiple DNA molecules are joined together; (c) loose flowerlike structures where, in some cases, strands of DNA are seen to be hanging out from one or both sides of the central core; (d) more compacted flowerlike structures with DNA strands more packed around the central core; (e) spheres or nanoparticles (of different size ranges); and (f) aggregated spheres (which is negligible in proportion). Table 1 shows the size range of the structures observed. We have calculated the proportion of these structures under each condition of complex formation for all six peptides (using the protocol mentioned in Methods). This is graphically represented in Figure 4. Both qualitative (Figure 3a) and quantitative (Figure 4; upper panel) AFM data reveal that, at the lower charge ratios (0.8 and 1.25), $K_9$, $K_{12}$ and $K_{16}$ interact with DNA to form a large number of linear rodlike structures belonging to category a (this constitutes around 60% of the total structures at charge ratio 1.25). Additionally, spheres (category e) and some interconnected linear structures (category b) are also present. At higher charge ratios of 1.75 and 5, complexes formed with $K_9$ show a decreased proportion of linear rods and increased proportion of more condensed species like spheres (category e) as well as condensed flowerlike structures (category d). In the case of $K_{12}$ and $K_{16}$, at similar charge ratios, a reduction in the proportion of linear structures occurs, along with increase in the proportion of interconnected linears (category b) as well as loose and condensed flowers (categories c and d). At higher charge ratio of 10, in $K_9$ and $K_{12}$, completely condensed spheres are observed, whereas for $K_{16}$, less compacted flowerlike morphologies and nanoparticles coexist even at charge ratio 10 showing incomplete condensation. Thus, although the nature of the structures formed at different charge ratios are similar in the case of all three lysine homopeptides, their proportions vary at different charge ratios. The efficiency of condensation also decreases with increasing peptide length in the lysine peptides. However, when the polyplexes were prepared with the arginine peptides, the proportion of linear rods is much lower at low charge ratio of 1.25 and further decreases with increase in length, from 40% for $R_9$ to 10% for $R_{16}$. Instead, there is a coexistence of interconnected linears (category b), loose flowers (category c), condensed flowers (category d) and spheres (category e) in varying proportions in all cases (Figure 4; lower panel). At charge ratio 5, more condensed structures like condensed flowers (category d) and spheres (category e) constitute the major population. At still higher charge ratio of 10, spherical nanoparticles are seen in all three cases indicating complete condensation of the DNA. The possible mechanism of origin of these different structures has been elaborated in the Discussion.

**Particle Size Determination.** Supplementary Figure 1 in the Supporting Information summarizes the sizes (hydrodynamic radii) and size distribution of the $K_9$, $K_{16}$, $R_9$ and $R_{16}$ polyplexes prepared at charge ratio 10. The sizes of both arginine polyplexes are almost similar, ranging from 64 to 70 nm, whereas the size of lysine polyplexes increases with peptide length from around 67 nm for $K_9$ to 86 nm for $K_{16}$. The bigger size and broad particle distribution of $K_{16}$ corresponds to its loose condensation state as seen from the AFM results.

**Stability of Polyplexes against Anionic Challenge.** Different anionic agents present extracellularly (glycosaminoglycans) and intracellularly (anionic polymers, proteins etc.) affect the stability of polyplexes on delivery. Such molecules have been an

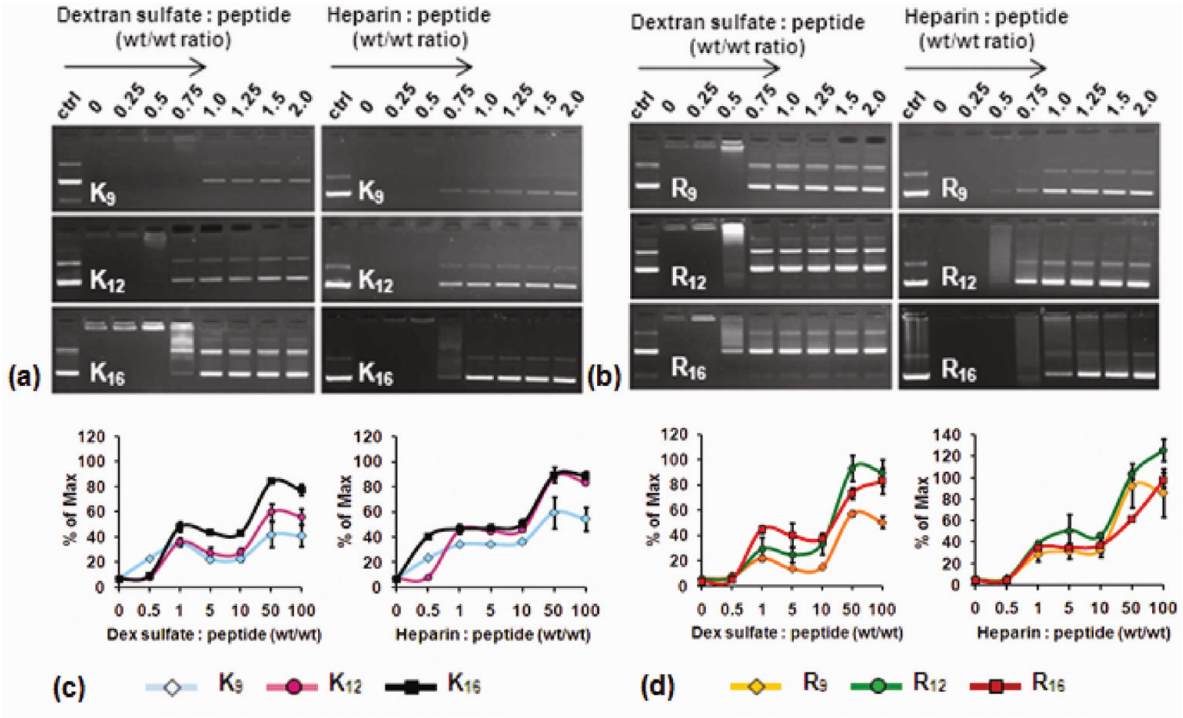


**Figure 5.** Gel and fluorimetry based DNA release assay showing relative stability of (a and c) lysine and (b and d) arginine polyplexes at charge ratio 10.0 against different anionic agents, dextran sulfate and heparin. In panels a and b lane 1 (ctrl) is uncomplexed plasmid DNA, lane 2 is respective polyplex at charge ratio 10 and lanes 3 to 9 are the polyplexes with dextran sulfate and heparin of different wt/wt ratios as indicated in the figure. In panels c and d the fluorescence of free uncomplexed DNA is set as maximum, i.e. 100%, and increase in fluorescence with increasing amount of anionic agent for different polyplexes is plotted at the *Y*-axis.

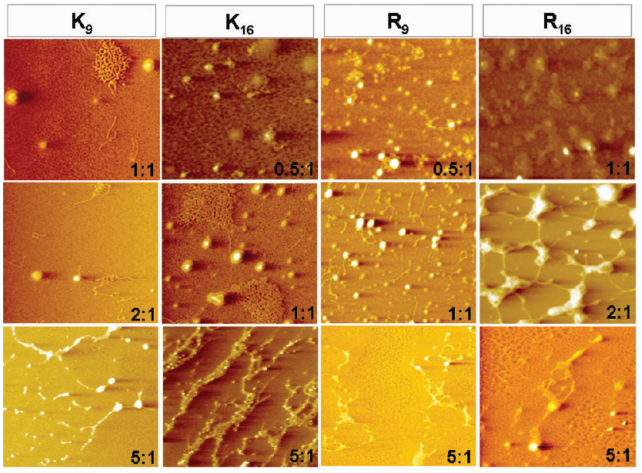


**Figure 6.** Representative AFM images of selected lysine and arginine polyplexes at charge ratio 10.0 on treatment with dextran sulfate at different weight/weight ratios. The release intermediates for $K_{12}$ and $R_{12}$ were also analyzed and show a pattern similar to that of their 9- and 16-mer counterparts. The images are not presented to avoid redundancy.

obvious choice for studying *in vitro* stability of peptide−DNA complexes.[28] In order to examine the relative stability of lysine and arginine polyplexes *in vitro*, we have challenged them with model anionic release agents like dextran sulfate and heparin at different concentrations. The amount of pDNA released from the destabilized polyplexes was estimated using agarose gel electophoresis and fluorimetry (Figure 5). The pattern of DNA release from the polyplexes was observed using AFM (Figure 6).

*a. DNA Release Using Gel Electrophoresis.* The release profile of pDNA and hence polyplex stability are different for the lysine and arginine polyplexes. $K_{16}$ polyplexes show complete release whereas $K_9$ and $K_{12}$ polyplexes release much less DNA in the presence of both the anionic agents (Figure 5a). Lysine polyplexes thus show decrease in stability with increase in peptide length. In comparison all the arginine polyplexes show significant DNA release: while the release is moderate in the case of $R_9$ and $R_{12}$, $R_{16}$ polyplexes show complete DNA release (Figure 5b).

*b. DNA Release Using Fluorimetry.* The DNA present in the condensed polyplexes at charge ratio 10 was not accessible for EtBr intercalation and thus showed negligible fluorescence. However when the polyplexes were subjected to an anionic challenge, they were destabilized (loosened structures or completely released DNA) and the relative amount of DNA released from the different polyplexes could be measured by addition of EtBr and monitoring the increase in fluorescence as shown in Figure 5c,d. In the case of the lysine polyplexes, the amount of DNA released on destabilization increases with increase in peptide length for both the anionic agents from 40% in the case of $K_9$ to 80% for $K_{16}$ (Figure 5c). For the arginine polyplexes, stability does not depend so strongly on peptide length since both $R_{12}$ and $R_{16}$ show more than 80% DNA release whereas in the case of $R_9$ it varies from 50% to 80% with dextran sulfate and heparin respectively (Figure 5d). In this assay we see an increase in fluorescence up to wt/wt ratio of 1.0 which further decreases slightly or remains constant until wt/wt ratio 10. This first plateau might indicate the presence of ternary complexes of

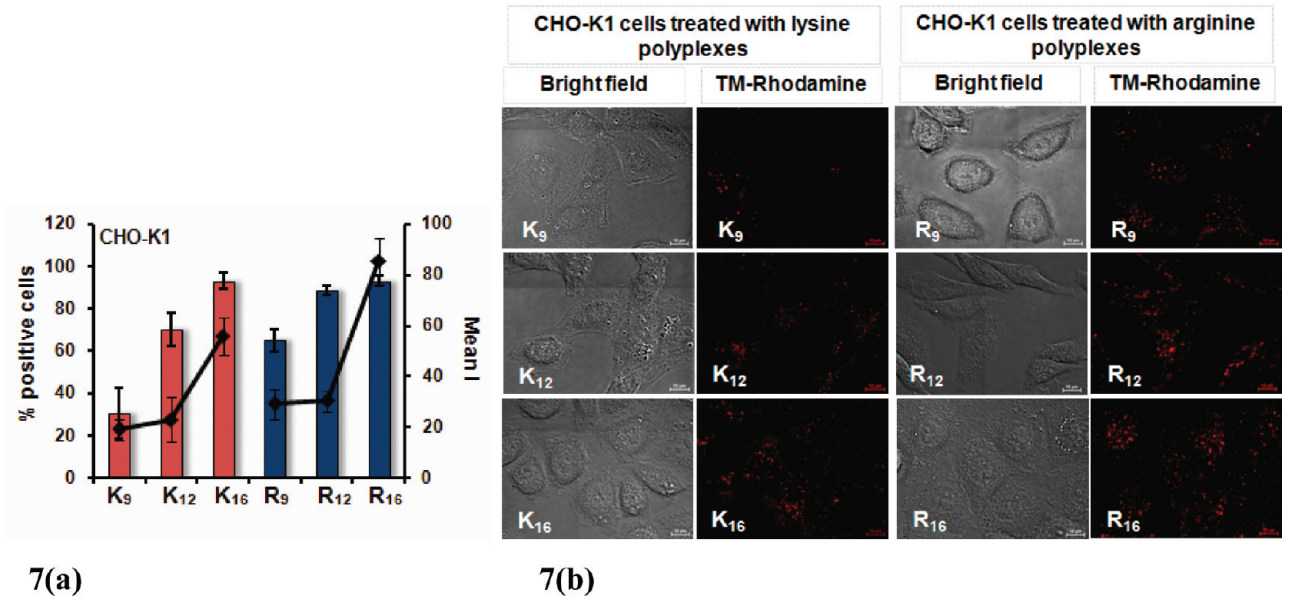


**Figure 7.** (a) Percentage of fluorescence positive cells (bars) and their mean intensity (line) measured using flow cytometry after 4 h incubation of the different polyplexes with CHO-K1 cells (where the DNA is labeled by TM-Rhodamine). (b) Bright field and TM- Rhodamine fluorescence microscopy images of the lysine and arginine polyplex treated CHO-K1 cells. The scale bar shown is of 10 $\mu$m.

partially relaxed polyplexes (which may be similar to the condensation intermediates in Table 1 albeit associated with the anionic agent) and anionic agent which resist further destabilization at these ratios but disassemble at higher amount of anionic agent. Such an effect cannot be seen in the gel release assay due to the instability of these ternary complexes under the gel running conditions.

**DNA Release from Polyplexes as Observed through AFM.** AFM has been used to further investigate the type of structures formed during the destabilization of polyplexes in the presence of dextran sulfate (Figure 6). The polyplexes formed at charge ratio 10 with each of the peptides were imaged in presence of different amounts of dextran sulfate. In the case of $K_9$, at the wt/wt ratio range of 1:1 to 2:1 (dextran sulfate:peptide) the AFM images indicate the presence of two types of structures: either free DNA (which are entangled in the image) or spherical structures of varying size (100−200 nm), usually larger than the nanoparticles present in the original polyplexes at this charge ratio. These particles are presumably some ternary complexes of $K_9$, DNA and dextran sulfate. At the highest wt/wt ratio of 5:1, interconnected free DNA strands are seen, along with some small particles indicating further release of pDNA from the nanoparticles and possible formation of peptide−dextran complexes. Similar structures are also seen in the images of $K_{16}$, where large spherical structures (>200 nm in size), small spheres (<100 nm in size) and bundles of free DNA are seen at 1:1, followed by more released DNA at 5:1.Thus, lysine polyplexes show two populations of particles on anionic challenge which are differently packed; some of the particles easily release DNA while the others are still in the complexed form. In contrast, polyplexes formed with $R_9$ and $R_{16}$ show partially loosened structures on anionic challenge at low wt/wt ratio (1:1). These structures resemble the loose flowerlike and interconnected structures seen in the AFM images of condensation of DNA with arginine peptides (charge ratio 0.8 to 5.0; Figure 3b). Further pDNA release is seen from all the structures at higher dextran amounts (2:1 and 5:1).

**Cellular Uptake of Polyplexes Using Flow Cytometry.** Cellular uptake studies were carried out using polyplexes prepared at $Z$ (±) of 10 where the DNA was labeled with TM-Rhodamine (TM-Rh), and the data is shown in Figure 7. It is observed that the percentage of fluorescence positive cells increases with peptide length in the case of the lysine polyplexes: only 30% of the cells are fluorescence positive for $K_9$, which increases to 70% for $K_{12}$ and 93% for $K_{16}$ (Figure 7a, bars). In comparison, even the lowest percentage of fluorescence positive cells is also quite high in the case of arginine polyplexes as seen in the case of $R_9$ (65%), while $R_{12}$ and $R_{16}$ show even higher TM-Rh positive cells (89% and 93% respectively). In addition, the mean fluorescence intensity plot (Figure 7a, line) shows that, in the case of lysine polyplexes, the mean intensities are rather low even where the percentage of fluorescence positive cells is high. For example, although $K_{12}$ has 2.3 times more positive cells than $K_9$, their mean intensities are similar. In comparison, the overall intensities are higher for all the arginine peptides, and the value is highest for $R_{16}$.

**Cellular Uptake of Polyplexes Using Fluorescence Microscopy.** We have tried to further corroborate these observations by fluorescence microscopy using TM-Rh labeled pDNA in the polyplexes (Figure 7b). Qualitative visualization indicates that $K_9$ has fewer fluorescent cells, which matches with the observations from flow cytometry. With increase in peptide length in the case of lysine, there is an increase in the number of cells showing TM-Rh fluorescence. However, the fluorescence patterns show cell-to-cell nonuniformity for all the lysine polyplexes. The cells treated with arginine polyplexes of all lengths show overall higher fluorescence as compared to lysine. We have also quantitated the sum intensity of fluorescence of around 50 cells (chosen from different fields) in each case and observed similar fluorescence distribution as in the case of flow cytomtery where $R_{16}$ shows highest intensity among all (data not shown).

**Intracellular State of the Polyplex.** The results described above indicate that both the percentage of cells and the intensity

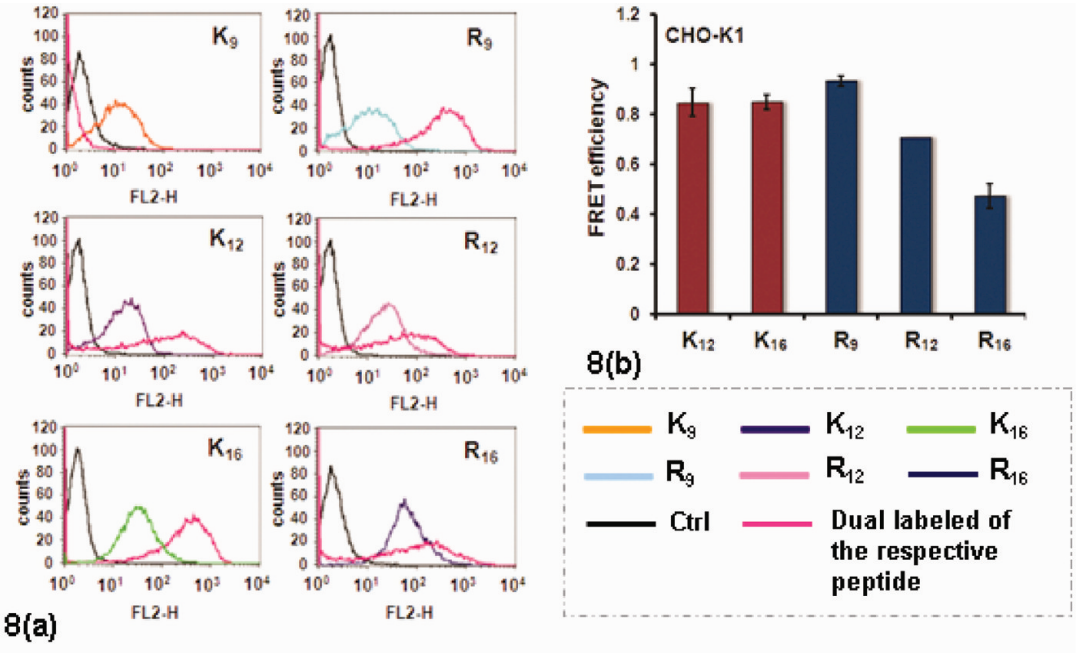


**Figure 8.** CHO-K1 cells were treated with single labeled (DNA labeled with TM-Rhodamine) and dual labeled (peptide labeled with FITC and DNA labeled with TM-Rhodamine) polyplexes for 4 h and analyzed on FACS caliber. Both FITC and TM-Rh were excited using a 488 nm laser. (a) TM-Rhodamine fluorescence intensity profile of the single and dual labeled polyplexes and (b) the FRET efficiency of the different polyplexes calculated using formula $[(F_d - F_s)/F_d]$, where $F_d$ and $F_s$ are the mean fluorescence intensity of TM-Rh positive cells treated with the dual labeled and single labeled polyplexes respectively.[24]

of fluorescence vary significantly depending upon whether lysine or arginine peptides are used in the polyplex. This can be attributed to a combined effect of differential polyplex uptake as well as differences in intracellular state of the two types of polyplexes. To explore this further, we used dual-labeled polyplexes (TM-Rh labeled pDNA and FITC labeled peptide) and carried out the flow cytometry experiments. Since the fluorophore pair chosen was a fluorescence resonance energy transfer (FRET) pair, we expected FRET to occur wherever the peptide and DNA molecules were in close proximity (≤10 nm), leading to energy transfer from the donor (FITC) to the acceptor (TM-Rh), thereby increasing the fluorescence intensity of the signal from the acceptor. The intensity profiles of the Rhodamine fluorescence of single labeled and dual labeled polyplexes are shown in Figure 8a, and the FRET efficiency values are plotted in Figure 8b (calculated as mentioned in Methods).

It is observed that, in the case of the lysine peptides $K_{12}$ and $K_{16}$, TM-Rh fluorescence intensity of the dual labeled polyplexes increases significantly in comparison to the single labeled, indicating that the peptide is still associated with the DNA intracellularly. $K_9$ polyplexes, which seem to be the most stable and show much less release among all polyplexes, were expected to show FRET maximally, but this is not observed. This apparent anomaly is possibly arising due to an overcompensation effect. The emission spectrum of FITC overlaps considerably with the TM-Rh emission spectra, so in the case of dual labeled polyplexes, a compensation is applied to remove the FITC fluorescence from the TM-Rh emission channel. In $K_9$ the number of fluorescent positive cells and the TM-Rh fluorescence intensity are very low as can be seen from Figures 7a and 8a, which results in a decrease in signal when compensation is applied, leading to erroneous results. Hence we have not included $K_9$ in our analysis. In the case of the arginine peptides, only $R_9$ polyplexes show an increase in fluorescence intensity in the dual labeled case as expected, since they are also slightly more compact and more stable against anionic challenge as compared to the other arginine polyplexes. FRET efficiency decreases further for $R_{12}$ and $R_{16}$. This suggests that arginine polyplexes ($R_{12}$ and $R_{16}$) can disassemble more easily under intracellular conditions.

## DISCUSSION

The first step in nonviral DNA delivery involves preparation of a vector−DNA complex in which the vector efficiently condenses DNA and also allows its appropriate intracellular release for transgene expression. Such condensation−release balance is likely to be dependent on the nature of the vector and its interaction with DNA. Our results point to some interesting comparisons between lysine and arginine polyplexes in this regard and show that the condensation and release mechanisms and efficiencies *in vitro* are dependent upon the chemistry and length of the carrier molecule, which in turn affects the cellular uptake and intracellular properties and thus transfection efficiency.

**Condensation of DNA Is Different for Lysine and Arginine Homopeptides.** In this study we have used L-lysine and L-arginine peptides of three different lengths to explore the effect of length and chemistry on the process of condensation and have proposed a possible mechanism of DNA condensation from our observation at the single molecule level at different charge ratios using AFM (Figure 9). It needs to be mentioned here that the images captured at each charge ratio are after equilibration of the complex for 30 min and are not kinetic intermediates of condensation. Nonetheless, they point toward fundamental differences between the pattern of DNA assembly of lysine and arginine peptides. The AFM images show that small rodlike structures (category a)

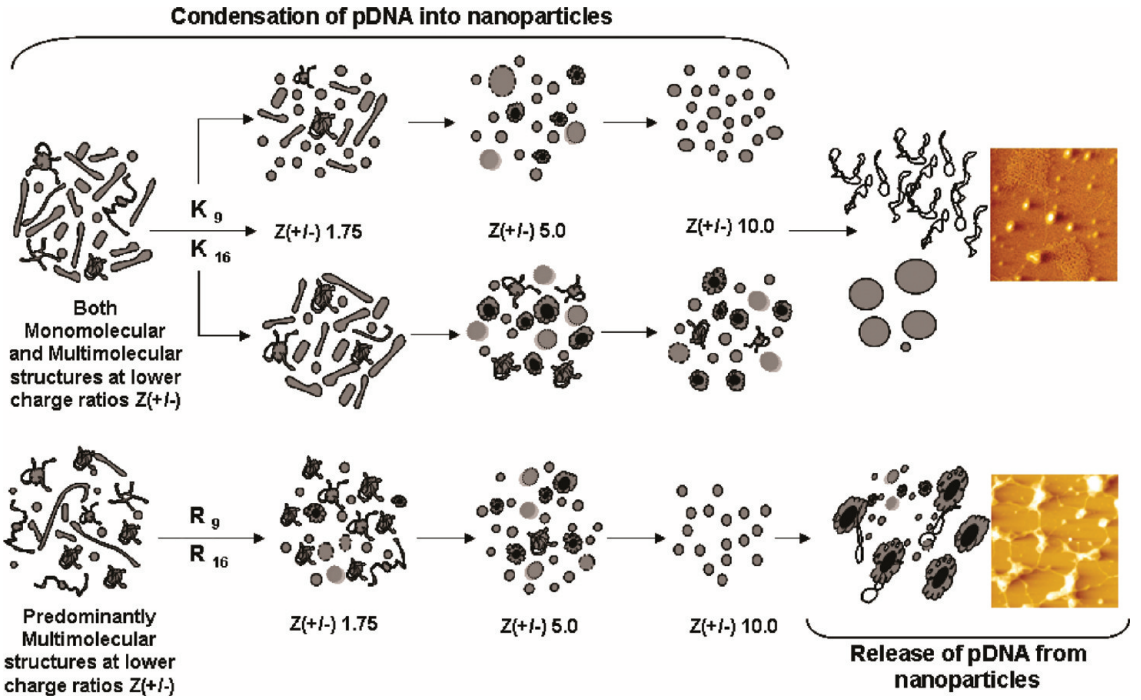


**Figure 9.** The proposed mechanism of pDNA condensation and release with L-lysine and L-arginine based homopeptides. Explanation of the symbols used is given in Table 1.

constitute the major molecular morphology when lysine peptides are used to make the polyplexes at lower charge ratios. These are possibly formed by monomolecular condensation through bending and folding of individual pDNA molecules as observed in an earlier study using poly-L-lysine. The longer structures (interconnected linears, category b) and loose flowers (category c) are likely to have formed through contacts among multiple pDNA molecules by the cationic peptide, i.e. they are condensed multimolecular structures. Figure 4 shows a preponderance of monomolecular structures at $Z$ (±) of 1.25 along with several multimolecular structures for lysine peptides, suggesting that they condense DNA in both monomolecular and multimolecular manner. The exact proportion of the monomolecular and multimolecular species at a particular charge ratio can vary depending upon the length of the peptide used as seen in Figure 4. However, in the case of arginine peptides, more multimolecular structures (categories b, c and d) are seen up to a charge ratio of 5.0 (Figure 4 lower panel). We have tried to rationalize this difference based on the fact that lysine and arginine bind to DNA in different ways.[29] Both lysine and arginine have the same positive charges, but the distribution of charge is different in the two cases as there is only one amine group in the lysine side chain whereas the guanidinium moiety in the arginine side chain has three amine groups. Although both lysine and arginine peptides can interact electrostatically with phosphate group of DNA, the mode of interaction could be different. The guanidinium moiety containing three amine groups allows zwitterion hydrogen bonding with the phosphate group of DNA thereby providing binding strength owing to its charge and structural organization. It is also known to form hydrogen bonds with bases like guanine and thus can interact with DNA in a variety of manners.[30] Additionally the guanidinium group is bulkier than the single amine group, which can hinder the interaction of its adjacent guanidinium groups to interact with the same DNA molecule by putting steric constraints and is likely to orient it in such a way that it can interact with another DNA molecule.[31] Thus arginine can favor the interaction of multiple DNA molecules thereby allowing the formation of multimolecular structures as seen in AFM images at low charge ratios. On the other hand there is only a single amine group in the lysine side chain, and less steric hindrance is expected in this case. Also it has been reported in the literature that lysine peptides can interact in a cooperative manner where the probability of a second peptide interacting with a lysine homopeptide-bound DNA is more than that with a free DNA molecule.[32] We have majorly observed monomolecular structures in the case of lysine homopeptides which can be explained by cooperative interactions. The cooperative interaction will result in two types of DNA populations: one having many lysine homopeptides attached to a single DNA molecule and the other of free DNA molecules which can form intermolecular contacts through the limited available cationic agent forming multimolecular structures. For arginine peptides, the complexes would assemble in a noncooperative manner. It has in fact been shown in the literature that, in DNA−polyarginine complexes, only partial cationic residues on polyarginine are effective for occupying DNA phosphate groups while all residues in polylysine are capable of occupying the DNA phosphate groups.[29]

***In Vitro* DNA Release from the Lysine and Arginine Polyplexes Correlates with Its Condensation.** The pattern of DNA release from the polyplexes also depends upon how they are packaged. This is seen when the lysine and arginine polyplexes at charge ratio 10 (the same charge ratio at which transfection was carried out) are challenged with dextran sulfate (Figure 6). It is difficult to quantitate the proportions of the different structures present in each condition because of the presence of multiple species like peptide−DNA complexes, peptide−DNA−dextran sulfate complexes, free DNA, free dextran sulfate and peptide−dextran

sulfate complexes depending on the relative amounts of all the components. However, it is clear from the images that, in the case of $K_9$ and $K_{16}$, few nanoparticles completely release DNA and few remain in the bound form, either with or without dextran sulfate attached to them. More particles seem to release DNA as the peptide length increases. This agrees with the condensation data, which points toward possible existence of multiple types of particles in lysine polyplexes. In the case of $R_9$ and $R_{16}$, there is gradual DNA release from all the condensed polyplexes (likely to be multimolecular in nature), which increases with increase in dextran sulfate, eventually leading to maximum release of DNA at the highest amount of dextran sulfate used.

**Lysine Peptides Show Stronger Length Dependence in DNA Condensation and Release than the Arginine Peptides.** Another difference that we observe through gel release and EtBr exclusion assays, particle size measurements and the AFM images is that, in the case of lysine homopeptides, 9-mer lysine condenses pDNA more strongly than the 12- and 16-mer lysine, thereby showing that the condensation efficiency for lysine peptides is dependent on the peptide length. Such an observation has been made by us in our earlier study as well where better condensation ability of the shortest polymer (19-mer poly-L-lysine) was observed at low DNA concentrations as compared to the longer counterparts (43-mer and 120-mer).[23] We do see some length dependence in the case of arginine peptides where $R_9$ shows higher stability than the longer arginine peptides, but here the binding of DNA with peptide is not so strong as with $K_9$ and $K_{12}$ (Figure 5). This could also be arising because of the differences in the condensation between the two. Condensation of DNA is a process that involves different interactions, and the energetics is governed by multiple forces. For example, there is a large loss of entropy on conversion of the long extended conformations of the DNA molecules to the packed morphology in the presence of highly charged cations. However, the process is still energetically favorable since there is a large energy gain on removal of the counterions already present on the DNA surface (which shield the inter-DNA charge−charge repulsions). In fact counterion fluctuations and hydration forces seem to be critical in determining the energetics of DNA condensation.[33] Our results seem to indicate that lysine homopeptides exhibit more cooperative interaction during condensation. Although cooperative interaction would mean more loss of conformational entropy of the DNA molecule because of bending and folding and subsequent condensation, the high energy gain on complete counterion release is likely to act as the driving force for condensation.[34] In the case of cooperative interaction as in the lysine peptides, such arrangement of the multiple peptides on single DNA molecules would be more easily achievable when the peptide length is smaller. Thus the condensation is stronger in lower length regimes and there is strong length dependence in the condensation process. In the case of arginine, the mechanism seems to be more in the noncooperative regime where multiple DNA molecules come together to form the complexes. In such a scenario, there would thus be less length dependence of condensation. Therefore both efficiency of condensation and its dependence on the peptide length seems to be controlled by the chemistry of the cationic agent. It also needs to be noted here that several literature reports show increase in condensation efficiency with increase in length of the carrier.[35,36] However, it is difficult to compare these results with ours since the experiments have been carried out with different length ranges and under different conditions (e.g., presence of salt and buffers) which can affect the electrostatic interactions.

**Uptake and Intracellular State of the Polyplex Depends on Its Condensation and Release Characteristics.** The differences in mechanism of DNA condensation and release in the lysine and arginine polyplexes are also reflected in their cellular uptake. The variations in the number and intensity of the fluorescence positive cells can arise due to differences in uptake of the TM-Rh labeled complexes over the entire cell population, because of inherent differences in polyplex characteristics as well as differences in the intracellular state of the polyplexes. Our biophysical experiments indicate toward a heterogeneous population in the case of the lysine polyplexes which can result in population of particles which are either very strongly condensed or weakly condensed resulting in low uptake and variability in cell-to-cell uptake. Such variation in uptake is observed in the fluorescence microscopy experiments also, particularly in the case of $K_9$. Moreover, when the complex is tightly packed even after entry (which is possible in the polyplexes made with $K_9$ showing poor *in vitro* DNA release), the number of cells which will count as fluorescence positive, as well as the intensity of fluorescence, is likely to be lower as compared to the case where the polyplex has already disassembled releasing free labeled DNA molecules (for example, in the case of $K_{16}$, which shows better release *in vitro*). This might be an additional factor contributing to the observed differences in the number and intensity of fluorescent positive cells in the lysine polyplexes. Higher uptake observed in the case of arginine polyplexes might be because of the homogeneous nature of the polyplexes. Arginine homopeptides and other cell penetrating peptides containing multiple arginines are also known to exhibit strong cellular uptake, which might be an additional contributing factor.[37,38]

In order to check for contribution of intracellular state of the polyplex on the uptake, we have carried out FRET assay using flow cytometry. Complexes made of cationic agents and DNA can undergo spontaneous intracellular unpackaging. After entry in the cells possibly through an endocytotic route, some of the bound polyplexes are possibly degraded by endosome−lysosome fusion. However, those polyplexes which can escape from the endosomes would undergo unpackaging in the presence of the different anionic triggers present in the cytosol like anionic proteins, RNA, sugars and so on. However, although the same triggers act on all the complexes, the relative destabilization would depend on the nature of the complex. This has been determined by the FRET assay. Higher FRET value is indicative of the condensed structure of polyplex within the cells. On the other hand, decreasing FRET signal indicates the unpackaging of the complex. The intracellular unpackaging of polyplexes has been generally explored in the literature using fluorescence microscopy based studies.[39,40] Compared to the conventional pixel-counting method using confocal microscopy, the flow cytometry based FRET analysis offers easier and more quantitative evaluation of unpackaging of the nucleic acid−vector complexes on large population.[24,41] In our study, *in vitro* experiments with lysine peptides show increasing DNA release with increase in peptide length, but the FRET intensity data for $K_{12}$ and $K_{16}$ shows strong FRET signal. This indicates that although unpackaging might occur as indicated clearly by the gel, EtBr assays and AFM data, there might be a population of particles which remains condensed and account for the strong FRET signal. We have not been able to get a correct estimate of the FRET intensity for the $K_9$ polyplex because of the effect of overcompensation which is a

limitation of the experiment. On the other hand, in the case of arginine, the FRET signal clearly decreases with increase in peptide length, indicating that there are indeed subtle differences in their intracellular state, where $R_{16}$ shows the least FRET signal indicating maximum dissociation of the polyplexes inside the cells.

**Differences in DNA Condensation and Release Account for the Differences in Transfection Efficiency between Lysine and Arginine.** The overall low transfection efficiency of the lysine peptides as compared to the arginine peptides could thus be arising because of different packaging modes adopted by lysine peptides which results in a heterogeneous population of particles, low uptake and different efficiencies of intracellular release. Even when the overall uptake is high as in the case of $K_{16}$, incomplete release of the DNA under the intracellular conditions (as indicated by the FRET experiments) might be responsible for the low transfection. In the case of arginine, single mode of DNA packaging, smaller particle size, and higher intracellular uptake along with good ability of DNA release particularly at higher peptide length make the overall transfection efficiency better than that of the lysine peptides. We would also like to add here that the 16-mer peptides of both lysine and arginine give better transfection in comparison with their shorter counterparts (9-mer and 12-mer) because of their better condensation and release balance.

**Implications in Future Vector Design.** Our study clearly demonstrates the importance of using arginine or guanidinium group in the DNA condensation moiety as compared to lysine because of the different mechanism of DNA assembly of arginine. However, it needs to be noted here that arginine and lysine homopeptides usually need to be modified with other functional moieties for improving their DNA delivery efficiency and better suitability for *in vivo* applications since their *in vivo* stability in unmodified form is not very high. Such modifications can be achieved by using a core−shell self-assembled system where such arginine based DNA condensing systems optimized for the DNA condensation and release balance can be used to form the condensed DNA core.[16] Also the arginine homopeptides can be modified with other appropriate amino acids which not only will impart multifunctionality in the system and help in overcoming different intracellular barriers more efficiently but also can show better compatibility *in vivo*. We are currently adopting the latter approach with the arginine peptides by modifying them with histidine and cysteine residues to impart other functionalities like endosomal escape, better particle stability and controlled intracellular release property. Our preliminary data for such systems shows that the trends observed in this study can be directly applied to such multifunctional peptides also. Further characterization of such systems which also have direct applicability *in vivo* is currently underway in our laboratory.

## ■ ASSOCIATED CONTENT

**Supporting Information.** Supplementary Figure 1 showing the mean size and size distribution profile of different polyplexes. Supplementary Figure 2, a schematic showing cooperative (upper panel; K) and noncooperative interactions (lower panel; R). This material is available free of charge via the Internet at http://pubs.acs.org.

## ■ AUTHOR INFORMATION

### Corresponding Author

*Institute of Genomics and Integrative Biology, Mall Road (near Jubilee Hall), Delhi 110007, India. E-mail: mganguli@igib.res.in, mganguli@igib.in. Tel: 091-11-27666156. Fax: 91-011-27667471.

## ■ ACKNOWLEDGMENT

This work was financially supported by Council of Scientific and Industrial Research (CSIR, NWP35) India; Swedish Research Council (VR-NT); SSF (Sweden−Japan); Center for Biomembrane Research, Stockholm, and Knut-Alice Wallenberg's Foundation. Fellowships from CSIR, India, and DBT, India, to A.M., V.S., G.T. and R.N. are acknowledged. Help from Anirban Kar and Vinod Yadav in microscopy experiments is acknowledged.

## ■ REFERENCES

(1) Edelstein, M. L.; Abedi, M. R.; Wixon, J. Gene therapy clinical trials worldwide to 2007—an update. *J. Gene Med.* **2007**, *9*, 833–842.

(2) Pouton, C. W.; Seymour, L. W. Key issues in non-viral gene delivery. *Adv. Drug Delivery Rev.* **2001**, *46*, 187–203.

(3) Mintzer, M.; Simanek, E. E. Nonviral vectors for gene delivery. *Chem. Rev.* **2009**, *109*, 259–302.

(4) Santos, J. L.; Pandita, D.; Rodrigues, J.; Pego, A. P.; Granja, P. L.; Balian, G.; Tomas, H. Receptor mediated gene delivery using PAMAM dendrimers conjugated with peptides recognized by mesenchymal stem cells. *Mol. Pharmaceutics* **2010**, *7* (3), 763–774.

(5) Mann, A.; Thakur, G.; Shukla, V.; Ganguli, M. Peptides in DNA delivery: current insights and future directions. *Drug Discovery Today* **2008**, *13*, 152–160.

(6) Morris, M. C.; Chaloin, L.; Heitz, F.; Divita, G. Translocating peptides and proteins and their use for gene delivery. *Curr. Opin. Biotechnol.* **2000**, *11*, 461–466.

(7) Gottschalk, S.; Sparrow, J. T.; Hauer, J.; Mims, M. P.; Leland, F. E.; Woo, S. L. A novel DNA peptide complex for efficient gene transfer and expression in mammalian cells. *Gene Ther.* **1996**, *3*, 448–57.

(8) Adami, C. R.; Collard, W. T.; Gupta, S. A.; Kwok, K. Y.; Bonadio, J.; Rice, K. G. Stability of peptide-condensed plasmid DNA formulations. *J. Pharm. Sci.* **1998**, *6*, 678–683.

(9) Dizhe, E. B.; Ignatovich, I. A.; Burov, S. V.; Pohvoscheva, A. V.; Akifiev, B. N.; Efremov, A. M.; Perevozchikov, A. P.; Orlov, S. V. Complexes of DNA with cationic peptides: conditions of formation and effecting internalization by mammalian cells. *Biochemistry (Moscow)* **2006**, *71*, 1350–1356.

(10) Parker, L.; Eckley, L.; Singh, S.; Preece, J. A.; Collins, L.; Fabre, J. W. $(LYS)_{16}$-based reducible polycations provide stable polyplexes with anionic fusogenic peptides and efficient gene delivery to post mitotic cells. *Biochim. Biophys. Acta* **2007**, *1770*, 1331–1337.

(11) Kim, H. H.; Lee, W. S.; Yang, J. M.; Shin, S. Basic peptide system for efficient delivery of foreign genes. *Biochim. Biophys. Acta* **2003**, *1640*, 129–136.

(12) Manickam, D.; Bisht, H.; Wan, L.; Mao, G.; Oupicky, D. Influence of TAT-peptide polymerization on properties and transfection activity of TAT/DNA polyplexes. *J. Controlled Release* **2005**, *102*, 293–306.

(13) Ferrer-Miralles, N.; Vazquez, E.; Villaverde, A. Membrane-active peptides for non-viral gene therapy: making the safest easier. *Trends Biotechnol.* **2008**, *26*, 267–275.

(14) Kim, J. B.; Choi, J. S.; Nam, K.; Lee, M.; Park, J. S.; Lee, J. K. Enhanced transfection of primary cortical cultures using arginine-grafted PAMAM dendrimer, PAMAM-arg. *J. Controlled Release* **2006**, *114*, 110–117.

(15) Futaki, S.; Ohashi, W.; Suzuki, T.; Niwa, M.; Tanaka, S.; Ueda, K.; Harashima, H.; Sugiura, Y. Sterylated arginine −rich peptides: a new class of transfection systems. *Bioconjugate Chem.* **2001**, *12*, 1005–1011.

(16) Kogure, K.; Akita, V.; Harashima, H. Multifunctional envelope-type nano device for non-viral gene delivery: concept and application of programmed packaging. *J. Controlled Release* **2007**, *122*, 246–251.

(17) Grigsby, C. L.; Leong, K. W. Balancing protection and release of DNA: tools to address a bottleneck of non-viral gene delivery. *J. R. Soc., Interface* **2010**, *7*, S67–S82.

(18) Hama, S.; Akita, H.; Ito, R.; Mizuguchi, H.; Hayakawa, T.; Harashima, H. Quantitative comparison of intracellular trafficking and

nuclear transcription between adenoviral and lipoplex systems. *Mol. Ther.* **2006**, *13*, 786–794.

(19) Schaffer, D. V.; Fidelman, N. A.; Dan, N.; Lauffenburger, D. A. Vector Unpackaging as a potential barrier for receptor - mediated polyplex gene delivery. *Biotechnol. Bioeng.* **1999**, *67*, 598–606.

(20) Hoggard, M. K.; Varum, K. M.; Issa, M.; Danielsen, S.; Christensen, B. E.; Stokke, B. T.; Artursson, P. Improved chitosan-mediated gene delivery based on easily dissociated chitosan polyplexes of highly defined chitosan oligomers. *Gene Ther.* **2004**, *11*, 1441–1452.

(21) Bertschinger, M.; Backliwal, G.; Schertenleib, A.; Jordan, M.; Hacker, D. L.; Wurm, F. M. Disassembly of polyethylenimine-DNA particles in vitro: implications for polyethylenimine-mediated DNA delivery. *J. Controlled Release* **2006**, *116*, 96–104.

(22) Mann, A.; Khan, M. A.; Shukla, V.; Ganguli, M. Atomic force microscopy reveals the assembly of potential DNA "nanocarriers" by poly-l-ornithine. *Biophys. Chem.* **2007**, *129*, 126–136.

(23) Mann, A.; Richa, R.; Ganguli, M. DNA condensation by poly-l-lysine at the single molecule level: role of DNA concentration and polymer length. *J. Controlled Release* **2008**, *125*, 252–262.

(24) Lee, H.; Kim, I. K.; Park, T. G. Intracellular trafficking and unpacking of siRNA/quantum dot-PEI complexes modified with and without cell penetrating peptide: confocal and flow cytometric FRET analysis. *Bioconjugate Chem.* **2010**, *21*, 289–295.

(25) Niidome, T.; Takaji, K.; Urakawa, M.; Ohmori, N.; Wada, A.; Hirayama, T.; Aoyagi, H. Chain length of cationic α- helical peptide sufficient for gene delivery into cells. *Bioconjugate Chem.* **1999**, *10*, 773–780.

(26) Hansma, H. G.; Golan, R.; Hsieh, W.; Lollo, C. P.; Mullen-Ley, P.; Kwoh, D. DNA condensation for gene therapy as monitored by atomic force microscopy. *Nucleic Acids Res.* **1998**, *26*, 2481–2487.

(27) Fang, Y.; Hoh, J. H. Early intermediates in spermidine-induced DNA condensation on the surface of mica. *J. Am. Chem. Soc.* **1998**, *120*, 8903–8909.

(28) Danielsen, S.; Strand, S.; Davies, C. D. L.; Stokke, B. T. Glycosaminoglycan destabilization of DNA−chitosan polyplexes for gene delivery depends on chitosan chain length and GAG properties. *Biochim. Biophys. Acta* **2005**, *1721*, 44–54.

(29) Ichimura, S.; Zama, M. Quantitative study of dye binding to DNA-polylysine and DNA-polyarginine complexes. *Biochem. Biophys. Res. Commun.* **1972**, *49*, 840–847.

(30) Vigneron, J. P.; Oudrhirit, N.; Fauquett, M.; Vergelyt, L.; Bradley, J. C.; Bassevillet, M.; Lehnt, P; Lehn, J. M. Guanidinium-cholesterol cationic lipids: efficient vectors for the transfection of eukaryotic cells. *Proc. Natl. Acad. Sci. U.S.A.* **1996**, *93*, 9682–9686.

(31) Tao, J.; Frankel, A. D. Specific binding of arginine to TAR RNA. *Proc. Natl. Acad. Sci. U.S.A.* **1992**, *89*, 2723–2726.

(32) Liu, G.; Molas, M.; Grossmann, G. A.; Pasumarthy, M.; Perales, J. C.; Cooper, M. J.; Hanson, R. W. Biological properties of poly-l-lysine-DNA complexes generated by cooperative binding of the polycation. *J. Biol. Chem.* **2001**, *276*, 34379–34387.

(33) Manning, G. S. The molecular theory of polyelectrolyte solutions with applications to the electrostatic properties of polynucleotides. *Q. Rev. Biophys.* **1978**, *11* (2), 179–246.

(34) Bloomfield, V. A. DNA condensation. *Curr. Opin. Struct. Biol.* **1996**, *6*, 334–341.

(35) Wadhwa, M. S.; Collard, W. T.; Adami, R. C.; McKenzie, D. L.; Rice, K. G. Peptide-mediated gene delivery: influence of peptide structure on gene expression. *Bioconjugate Chem.* **1997**, *8*, 81–88.

(36) Ziady, G.; Ferkol, T.; Dawson, D. V.; Perlmutter, D. H.; Davis, P. B. Chain length of the polylysine in receptor-targeted gene transfer complexes affects duration of reporter gene expression both *in vitro* and *in vivo*. *J. Biol. Chem.* **1999**, *274*, 4908–4916.

(37) Futaki, S.; Suzuki, T.; Ohashi, W.; Yagami, T.; Tanaka, S.; Ueda, K.; Sugiura, Y. Arginine-Rich Peptides, An Abundant Source of Membrane-Permeable Peptides having Potential as Carriers for Intracellular Protein Delivery. *J. Biol. Chem.* **2001**, *276*, 5836–5840.

(38) Mae, M.; Langel, U. Cell-Penetrating Peptides as Vectors for Peptide, Protein and Oligonucleotide Delivery. *Curr. Opin. Pharmacol.* **2006**, *6*, 1–6.

(39) Matsumoto, Y.; Itaka, K.; Yamasoba, T.; Kataoka, K. Intranuclear Fluorescence Resonance Energy Transfer Analysis of Plasmid DNA Decondensation from Nonviral Gene Carriers. *J. Gene Med.* **2009**, *11*, 615–623.

(40) Chen, H. H.; Ho, Y. P.; Jiang, X.; Mao, H. Q.; Wang, T. H.; Leong, K. W. Quantitative Comparison of Intracellular Unpacking Kinetics of Polyplexes by a Model Constructed from Quantum Dot-FRET. *Mol. Ther.* **2008**, *16*, 324–332.

(41) Breunig, M.; Lungwitz, U.; Liebl, R.; Goepferich, A. Fluorescence Resonance Energy Transfer: Evaluation of the Intracellular Stability of Polyplexes. *Eur. J. Pharm. Biopharm.* **2006**, *63*, 156–165.